MOISTURE CONTENT ESTIMATION OF HETEROGENOUS POROUS STONES USING HYPERSPECTRAL IMAGING

Danish Ali Chaghdo[1,2], Bikram Koirala[2], Laurent Fontaine[1], Tim De Kock[3], Roald Hayen[1], Paul Scheunders[2]

[1] Monuments and Monumental Decoration Lab, Royal Institute for Cultural Heritage (KIK-IRPA)
[2] Imec-Visionlab, Department of Physics, University of Antwerp (CDE), Universiteitsplein 1, B-2610 Antwerp
[3] Antwerp Cultural Heritage Sciences, University of Antwerp, Mutsaardstraat 31, 2000, Antwerp

ABSTRACT

Understanding how moisture interacts with porous building stones is essential for preserving heritage structures. Due to the strong absorption bands of molecular water in the short-wave infrared (SWIR) range, the spectral reflectance of moist samples is heavily influenced by water, enabling non-invasive monitoring via hyperspectral imaging. A recent dataset captured the spectral behavior of six types of stone at multiple moisture levels using high-resolution SWIR imaging. While the Normalized Relative Arc Length (NRAL) method effectively estimated moisture content in most samples, notable inaccuracies emerged for two specific limestones with strong internal heterogeneity, Euville and Savonnières. Petrographic thin-section analysis confirmed that a single hyperspectral pixel can indeed span both a large pore (wet region) and the surrounding stone matrix (dry region). To tackle this challenge, in this study, we present NRAL+, an enhanced method for modeling spectral reflectance as a mixture of dry and wet components at the sub-pixel level. The experimental results demonstrate the potential of the proposed approach.

Index Terms— Moisture Content, SWIR Hyperspectral Imaging, Sub-pixel Moisture Heterogeneity, Petrographic Analysis

1. INTRODUCTION

Stone materials used in historic buildings are especially prone to deterioration caused by a range of environmental and physical processes, including salt crystallization, freeze–thaw fluctuations, biological colonization, and chemical weathering. These mechanisms contribute both to the physical weakening and the visual degradation of heritage structures [1]. A primary factor that intensifies these decay processes is the elevated moisture content within the stone. Therefore, accurate measurement of moisture content (MC) is essential for diagnosing damage and developing informed conservation strategies. Various methods have been developed to quantify MC, encompassing both destructive and non-destructive techniques. Among the invasive methods, the gravimetric and calcium carbide approaches are widely used for their high precision and repeatability [2]. Nevertheless, due to their destructive nature, these techniques are often unsuitable in heritage contexts where material preservation is critical. To address this, a number of non-invasive techniques have been successfully implemented, allowing for moisture assessment while maintaining the integrity of the historic fabric. These include infrared thermography (IRT) [3], electrical resistivity tomography (ERT) [1], and nuclear magnetic resonance (NMR) [4].

The use of Hyperspectral Imaging (HSI) has emerged as a promising tool for investigating moisture content (MC) in building materials, particularly within the conservation of built heritage (BH). By capturing detailed spectral information across a wide range of wavelengths, HSI enables surface-level analysis that can reveal the spatial distribution of water and provide quantitative moisture estimates [5]. Despite its potential, HSI remains underutilized in heritage science. Only a few studies have specifically explored its application in this context. For instance, Liang et al. [6] demonstrated how SWIR bands at approximately 1.4 μm and 1.9 μm, wavelengths strongly absorbed by water,can be used to track moisture in wall structures. Building on this, Kogou et al. [7] advanced a hybrid strategy combining SWIR spectral imaging with remote Raman spectroscopy and machine learning to map both moisture and salt content in historical buildings. In another recent development, Chaghdo et al. [8] employed HSI to noninvasively quantify MC in various natural and historical stone types at multiple saturation levels. However, the reliability of HSI for moisture estimation is complicated by several material-dependent and environmental factors. The reflectance signals captured by HSI are significantly influenced by the porous structure of the material, pore size variation, and external conditions such as ambient humidity and temperature [9, 10]. Moreover, HSI is inherently limited to analyzing only the superficial layer of the material,typically just 100–300 μm deep, which may not reflect the moisture distribution within the bulk material [11]. In [11], a methodology was proposed to tackle these challenges. The approach estimates the MC of a sample from its relative position on the arc connecting two endmembers

(a dry and a fully saturated sample). In [8], this approach was successfully applied to estimate the MC of several stone types. While the approach yielded encouraging results for four stone types, it showed significantly higher errors for two stone types: Euville and Savonnières. These inaccuracies were mainly due to the high heterogeneity of these materials, in which wet and dry micro-regions coexist within a single pixel. The measured reflectance reflects contributions from both dry and wet regions in these scenarios. To address this challenge, the influence of the dry region on the measured signal must be accounted for. This study aims to develop a robust methodology that effectively deals with these limitations, allowing accurate MC estimation even in stones with complex and non-uniform internal moisture distributions. The remainder of the paper is organized as follows: the experimental data and methodology are presented in Section 2, results and discussion are detailed in Section 3, and conclusions are drawn in Section 4.

2. MATERIALS AND METHOD

2.1. Experimental Dataset

In [8], we prepared an extensive short-wave infrared (SWIR) hyperspectral dataset to characterize porous building materials under varying moisture conditions. The dataset was constructed from six different types of building stones: Euville, Massangis, Neubrunner, Obernkirchener, Savonnières, and red brick. For each stone type, six replicate cube samples (6x6x6 cm^3) were prepared, resulting in a total of 36 samples. All samples were initially fully saturated according to the NBN EN 1936:2007 standard procedure. Moisture content (MC) was then gradually reduced to establish six distinct levels: 100%, 90%, 75%, 50%, 25%, and 0%. Each sample was scanned using a Snapscan SWIR hyperspectral camera, having a spatial resolution of 500 µm, producing a benchmark hyperspectral dataset that captures the spectral signatures of the stones across varying moisture states. The dataset was analyzed using the Normalized Relative Arc Length (NRAL) [11] method, which yielded strong performance overall. However, reduced accuracy was observed for the Euville and Savonnières stone types, likely due to pixel-level heterogeneity, specifically, each hyperspectral pixel may encompass both dry and wet regions. To test this hypothesis, the present study investigates these two stone types in greater depth. For this purpose, 30 µm thin sections were prepared and analysed with a polarizing microscope (Axioplan, Zeiss) equipped with a digital camera (Invenio 5D II, DeltaPix). The thin sections were pre-impregnated under vacuum with yellow-colored epoxy resin to enhance the visualization of pores ranging from 50 to 500 µm.

2.1.1. Savonnières limestone

The following observations summarize the main petrographic features identified in the Savonnières samples: Savonnières is an oolitic limestone whose grains are held together by a dog-tooth sparite cement (see Fig. 1 for a general and a detailed view of the thin section). Most of the micritic oolites appear hollow since their nucleus was dissolved during diagenesis Fig. 1(b). As described by Roels et al.[12], the pore

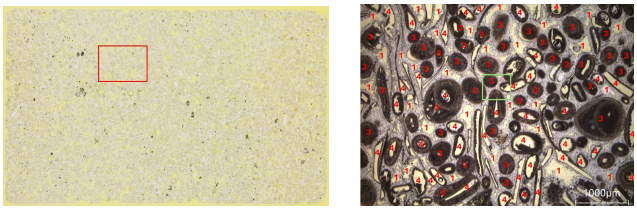

(a) (b)

Fig. 1. (a) General view of the thin-section of Savonnières stone (single shot taken using a light table and a camera); (b) Detail view showing the general appearance of Savonnières stone under a polarizing microscope (single polarized light). 1 = intergranular pores; 2 = intracrystalline pores of the sparite cement (in white); 3 = intragranular pores of the oolites and other stone grains; 4 = intragranular pores inside the oolites. The green grid box represents the area covered by a single pixel from the hyperspectral image.

structure of Savonnières limestone can be classified into four main categories. The first category is the intergranular pores that correspond to incompletely filled pore spaces (1, in yellow) between the grains. The second category concerns the intercrystalline pores of the sparite cement (2). The third and fourth category are the two types of intragranular pores: the very fine pores inside the concentric layers of the oolites and other types of stone grains (3), and the large moldic pores corresponding to the dissolution of the nuclei of the oolites (4). Pores of category (1) and (4) are very large and are the main contributors to the effective porosity, while the pores of category (2) and (3) are rather very small (limited contribution to effective porosity).

Since a significant amount of moisture in moist Savonnières resides in intergranular and large moldic pores, the distribution of these pores within the sample influences the measured hyperspectral data set. To visually demonstrate that a single hyperspectral pixel can indeed encompass both wet regions (intergranular and large moldic pores) and relatively dry regions (fine intragranular pores and intercrystalline pores within the sparite cement) of Savonnières, we overlay one pixel from the hyperspectral image (indicated by the green grid box) onto the microscopic image of the thin section in Fig. 1(b). As expected, a single hyperspectral pixel can overlap a part of a large pore (wet region) and a part of the stone material itself (dry region). We emphasize that this behavior

is consistent across the sample; the same observation holds true if the green grid box 1(b) is translated to any other location within the microscopic image of the thin section.

2.1.2. Euville limestone

The Euville samples were similarly analyzed, with the main petrographic characteristics outlined below. Euville is a crinoidal limestone whose grains are held together by a thick sparite cement (well-developed calcite) in optical continuity with crinoid ossicles (see Fig. 2 for a general and a detailed view of the thin section). Other grains can be identified as peloids and/or shell fragments with thin micrite envelopes Fig. 2 (b)). Three main categories of pores can be distinguished. The first category is the intergranular pores corresponding to the yellow coloured spaces (see detail view of the thin-section). These intergranular pores are the main contributors to the effective porosity of the stone. The second category concerns intragranular pores (i.e. pores inside the stone grains themselves) and the third category concerns intercrystalline pores (i.e. pores between the sparite crystals of the binder). The contribution of these last two categories of pores to the effective porosity is limited compared to the intergranular pores (first category).
Similar to Savonnières, a hyperspectral pixel (see the green grid box in Fig. 2 (b)) can cover both wet regions (intergranular pores) and relatively dry regions (intragranular pores and intercrystalline pores of the sparite cement) of Euville, further confirming the need to account for this effect when accurately estimating the MC of moist stone samples.

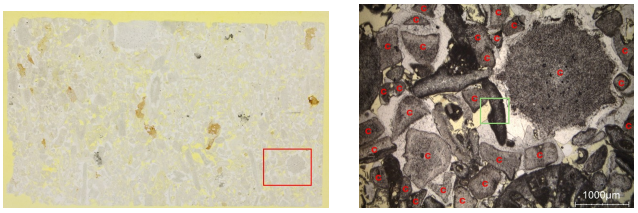

(a) (b)

Fig. 2. (a) General view of the thin-section of Euville stone (single shot taken using a light table and a camera); (b) Detail view showing the general appearance of Euville stone under a polarizing microscope (single polarized light). The intergranular pores can be seen in yellow. In this picture, the crinoid ossicles (C) appear light gray and are covered by overgrowths of sparite (in white). Most of the other stone grains appear dark gray or black. The green grid box represents the area covered by a single pixel from the hyperspectral image.

2.2. Methodology

The petrographic analysis reveals that big pores and dry micro-regions can coexist within a single pixel. In that case, its spectral reflectance can be modeled as a linear mixture of the spectral reflectance of dry ($\mathbf{R}_{dry}$) and wet ($\mathbf{R}_{wet}$) regions.

$$\mathbf{R} = (1-a)\mathbf{R}_{dry} + a\mathbf{R}_{wet} \tag{1}$$

where a denotes the fractional abundance of the wet region. The spectral reflectance of the wet region will be modeled as a two-layer model comprising stone grains and water. Water is a non-diffusely reflecting material, whereas the stone grains reflect incident light diffusely. Because of this, the thickness of the water layer (t) covering the stone grains can be related to the spectral reflectance of the wet region using the following physical model ([13]):

$$\mathbf{R}_{wet} = \mathbf{R}_{dry}\exp(-2\alpha t) \tag{2}$$

where α is the absorption spectrum of water.

To allow the MC estimation of the sample, the parameters t and a must be retrieved from the measured reflectance spectra, which can be done by inverting Eq. (1). This can be achieved by minimizing the difference between the observed and modeled reflectance spectra:
$\left|\left|\mathbf{R} - \mathbf{R}_{dry}\left[(1-a) + a\exp(-2\alpha t)\right]\right|\right|$, subject to the constraints, $t \geq 0$ and $0 \leq a \leq 1$. Variations in illumination and acquisition conditions often introduce scaling effects in the measured spectra. This can be dealt with by minimizing:
$\left|\left|\frac{\mathbf{R}}{||\mathbf{R}||} - \frac{\mathbf{R}_{dry}}{||\mathbf{R}_{dry}||}\left[(1-a) + a\exp(-2\alpha t)\right]\right|\right|$
where the function $||\cdot||$ denotes the Euclidean norm, which computes the length (magnitude) of the vector.

If the area that is covered by each pixel is known, the estimated thickness of the water layer in a pixel can be related to the volume of the water it contains (and thus the mass). When water is not uniformly distributed within a pixel, the thickness is influenced by dry regions within the pixel, and is on average given by:

$$t_{Avg} = a \times t \tag{3}$$

Within a unit volume, the maximum possible MC is contained in a fully saturated sample, corresponding to the maximum t_{Avg}. This correspondence allows us to define a relative measure of moisture based on water thickness. The t_{Avg} of a moist sample relative to that of the saturated sample serves as a proxy for MC. The MC of the moist sample can then be estimated by calibrating this proxy with the MC of the saturated sample:

$$\text{MC}(\mathbf{R}) = \frac{t_{Avg}(\mathbf{R})}{t_{Avg}(\mathbf{R}_{sat})} \times \text{MC}(\mathbf{R}_{sat}) \tag{4}$$

where $\mathbf{R}_{sat}$ denotes spectral reflectance of the saturated sample and MC $(\cdot)$ represents the MC of a sample.

In the following, we will refer to this method as NRAL+.

3. RESULTS AND DISCUSSION

Scatter plots comparing MC versus estimated MC for Euville and Savonnières stones, are shown in Fig 3. Two estimation methods are shown: NRAL(blue) and NRAL+(red). Reference lines include a solid red 1:1 line and dashed black $\pm 2g/g \times 100$ margin lines to evaluate estimation accuracy. Root Mean Square Error (RMSE) values for each method are displayed in the Table 1, highlighting the performance of NRAL and NRAL+ in estimating moisture content in these two porous building stones.

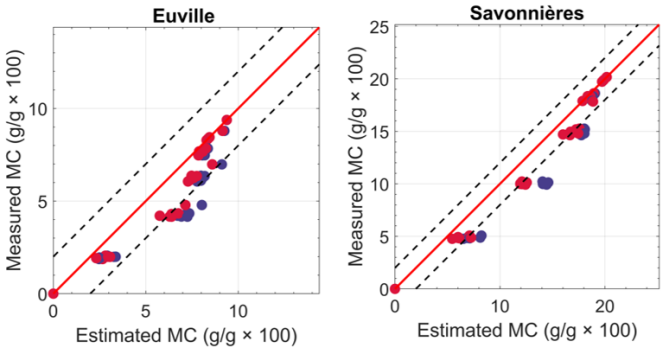

Fig. 3. Scatter plots of measured vs estimated moisture content for Euville and Savonnières stones comparing NRAL (blue) and NRAL+ (red).

Stone Type	RMSE NRAL	RMSE NRAL+
Euville	1.48	1.10
Savonniéres	2.38	1.35

Table 1. RMSE comparison between NRAL and NRAL+ for Euville and Savonnières stone types.

As shown in Fig. 3, the enhanced NRAL+ method, an improved version of NRAL, demonstrates a notable reduction in moisture content estimation errors for stone types in which wet and dry micro-regions coexist within a single pixel of a moist sample. The algorithm is particularly effective in addressing the challenges posed by such intra-pixel moisture heterogeneity, leading to a greater reduction in RMSE for Savonnières, where this phenomenon is more prevalent. This is supported by the results in Table 1, which show a comparatively smaller error reduction for Euville, where mixed wet–dry regions occur less frequently.

4. CONCLUSION

In this study, we developed NRAL+, an improved spectral unmixing method for estimating moisture content (MC) in porous stones affected by intra-pixel heterogeneity. NRAL+ models the observed reflectance as a linear combination of dry and wet micro-regions, where the wet component is physically described by a two-layer model comprising stone grains and an overlying water film. By inverting this model, NRAL+ retrieves the fractional wet area and water film thickness, enabling accurate MC estimation. Results show reduced scatter and RMSE values, especially for Savonnières, where mixed wet–dry regions are more frequent. Petrographic analysis supports these findings, confirming the presence of microscale heterogeneity. This consistency highlights NRAL+'s effectiveness in addressing spectral variability and improving non-destructive moisture assessment in stones.

Acknowledgement

This research was funded by the Belgium Science Policy (Belspo) within the framework of BRAIN-be 2.0, Belgian Research Action through Interdisciplinary Networks: project B2/212/P2/CLIMPACTH. Bikram Koirala is a postdoctoral fellow of the Research Foundation Flanders, Belgium (FWO: 1250824N-7028).

5. REFERENCES

[1] C. Alves, C. A. Figueiredo, J. Sanjurjo-Sánchez, and A. C. Hernández, "Effects of water on natural stone in the built environment—a review," *Geosciences*, vol. 11, no. 11, p. 459, 2021.

[2] D. Camuffo and C. Bertolin, "Towards standardisation of moisture content measurement in cultural heritage materials," *E-Preserv. Sci*, vol. 9, pp. 23–35, 2012.

[3] A. Moropoulou, K. C. Labropoulos, E. T. Delegou, M. Karoglou, and A. Bakolas, "Non-destructive techniques as a tool for the protection of built cultural heritage," *Construction and Building Materials*, vol. 48, pp. 1222–1239, 2013.

[4] D. Capitani, V. Di Tullio, and N. Proietti, "Nuclear magnetic resonance to characterize and monitor cultural heritage," *Progress in Nuclear Magnetic Resonance Spectroscopy*, vol. 64, pp. 29–69, 2012.

[5] M. Manley, "Near-infrared spectroscopy and hyperspectral imaging: non-destructive analysis of biological materials," *Chemical Society Reviews*, vol. 43, no. 24, pp. 8200–8214, 2014.

[6] H. Liang, "Advances in multispectral and hyperspectral imaging for archaeology and art conservation," *Applied Physics A*, vol. 106, pp. 309–323, 2012.

[7] S. Kogou, Y. Li, C. Cheung, X. Han, F. Liggins, G. Shahtahmassebi, D. Thickett, and H. Liang,

"Ground-based remote sensing and machine learning for in situ and noninvasive monitoring and identification of salts and moisture in historic buildings," *Analytical Chemistry*, 2025.

[8] D. A. Chaghdo, B. Koirala, L. Cristina, R. Hayen, and P. Scheunders, "Exploring the potential of hyperspectral imaging to estimate the moisture content in natural and historical stones," in *2024 14th Workshop on Hyperspectral Imaging and Signal Processing: Evolution in Remote Sensing (WHISPERS)*. IEEE, 2024, pp. 1–5.

[9] D. Camuffo, "Physical weathering of stones," *Science of the total environment*, vol. 167, no. 1-3, pp. 1–14, 1995.

[10] B. Menéndez, "Non-destructive techniques applied to monumental stone conservation," *Non-destructive testing*, 2016.

[11] B. Koirala, Z. Zahiri, and P. Scheunders, "A robust supervised method for estimating soil moisture content from spectral reflectance," *IEEE Transactions on Geoscience and Remote Sensing*, vol. 60, pp. 1–13, 2022.

[12] S. Roels, J. Carmeliet, H. Hens, and J. Elsen, "Microscopic analysis of imbibition processes in oolitic limestone," *Geophysical Research Letters*, vol. 27, no. 21, pp. 3533–3536, 2000.

[13] B. Koirala, N. Mboga, R. Moelans, E. Knaeps, S. Sels, F. Winters, S. Samsonova, S. Vanlanduit, and P. Scheunders, "Study on the potential of oil spill monitoring in a port environment using optical reflectance," *Remote Sensing*, vol. 15, no. 20, 2023. [Online]. Available: https://www.mdpi.com/2072-4292/15/20/4950